



HAL
open science

Stoichiometric and Catalytic Reduction of Carbon Dioxide by a Sterically Encumbered Amidinato Magnesium Hydride

Wimonsiri Huadsai, Laure Vendier, Helmar M Görls, Lionel Magna, Sébastien Bontemps, Matthias Westerhausen

► **To cite this version:**

Wimonsiri Huadsai, Laure Vendier, Helmar M Görls, Lionel Magna, Sébastien Bontemps, et al.. Stoichiometric and Catalytic Reduction of Carbon Dioxide by a Sterically Encumbered Amidinato Magnesium Hydride. *European Journal of Inorganic Chemistry*, In press, pp.e202400128. 10.1002/ejic.202400128 . hal-04632394

HAL Id: hal-04632394

<https://hal.science/hal-04632394>

Submitted on 2 Jul 2024

HAL is a multi-disciplinary open access archive for the deposit and dissemination of scientific research documents, whether they are published or not. The documents may come from teaching and research institutions in France or abroad, or from public or private research centers.

L'archive ouverte pluridisciplinaire **HAL**, est destinée au dépôt et à la diffusion de documents scientifiques de niveau recherche, publiés ou non, émanant des établissements d'enseignement et de recherche français ou étrangers, des laboratoires publics ou privés.



Distributed under a Creative Commons Attribution - NonCommercial - NoDerivatives 4.0 International License

Hot Paper

Stoichiometric and Catalytic Reduction of Carbon Dioxide by a Sterically Encumbered Amidinato Magnesium Hydride

Wimonsiri Huadsai,^[a, b] Laure Vendier,^[a] Helmar Görls,^[b] Lionel Magna,^[c] Sébastien Bontemps,^{*[a]} and Matthias Westerhausen^{*[b]}

A sterically encumbered dinuclear amidinato magnesium hydride **3** with bridging hydrido ligands was synthesized from the metalation of the corresponding amidine **1** with dibutylmagnesium and subsequent treatment with phenylsilane. This complex reacts stoichiometrically with 1 atm of carbon dioxide at room temperature in tetrahydrofuran (THF) to the corresponding bis(thf) adduct of the dinuclear formate complex **4-2thf** with bridging formate anions. This complex is stable in

THF at 60 °C for more than 16 hours but decomposes into the amidine **1** upon removal of ligated thf ligands. Complex **3** efficiently catalyzes the reduction of carbon dioxide with 9-BBN, yielding bis(boryl)acetal (R₂BO)₂CH₂, and with silanes H_{4-n}SiPh_n (n = 1, 2, and 3). The bis(silyl)acetal is quantitatively accessible for Ph₃SiH (n = 3) whereas during the reduction of CO₂ with hydrogen-rich silanes (n = 1, 2) siloxanes form and methane evolves.

Introduction

The chemistry of carbon dioxide is explored because its abundance would make it an important C₁ building block in synthetic chemistry. Therefore, its properties in coordination chemistry^[1] and its use in stoichiometric and catalytic reduction processes^[2] are important topics. Global abundance and non-toxicity of the alkaline-earth metals Mg and Ca elicit a vivid development of their reagents for stoichiometric and catalytic applications.

Since the discovery of organomagnesium compounds, these organometallics attract a large interest in organic, organometallic, catalytic, and coordination chemistry. The quite polar Mg–H bonds make the hydrides rather strong nucleophiles and reducing reagents, which usually can safely be handled in ethereal solvents. Besides the high reactivity, aggregation and ligand redistribution reactions (leading to Schlenk-type equilibria) can cause rather complex mixtures in solution, intercon-

verting hetero- into homoleptic compounds. To suppress these redistributions the metal center can be shielded by very bulky ligands to stabilize heteroleptic molecules. This strategy hinders far-reaching aggregation of hydrido magnesium complexes despite the fact that Mg-bound hydrido ligands avoid terminal binding modes and are commonly observed as bridging ligands.^[3] However, application of an extremely bulky β-diketiminato ligand stabilizes a mononuclear hydrido magnesium derivative which is highly moisture sensitive and hydrolysis occurs even in the crystalline state yielding the corresponding hydroxide under liberation of hydrogen and maintenance of crystallinity.^[4] In addition, strong Lewis bases such as DMAP are able to deaggregate the dinuclear hydrido magnesium complexes.^[5]

Bulky amidinato ligands represent alternatives to the shielding β-diketiminato ligands to study the reactivity of heteroleptic hydrido magnesium compounds toward carbon dioxide.^[6] Amidinates are bidentate anions with the possibility to enhance the shielding capability by bulky N-bound substituents and by addition of alkyl, aryl, or amino groups at the backbone. Thus, a number of sterically encumbered amidinato anions have been developed to suppress ligand scrambling and to protect the metal-centered reactive site.^[7] Sterically demanding N-bound 2,6-diisopropylphenyl (Dipp)^[8] and 2,6-dimesitylphenyl groups^[9] can hinder Schlenk-type ligand redistribution reactions and hence formation of homoleptic bis(amidinato) magnesium and calcium complexes. However, the group at the carbon backbone plays a key role. Aryl substituents (benzamidinates) and methyl groups (acetamidinates) at the carbon atom of the 1,3-diazaallyl backbone are not bulky enough and homoleptic magnesium bis(amidinate)s have been isolated.^[10] The more demanding *tert*-butyl group is required to safely suppress the formation of homoleptic alkaline-earth metal bis(amidinate)s of Mg and Ca and to stabilize heteroleptic amidinato compounds.^[11] In all these Mg complexes, the amidinato ligands have *syn*-conformation and bind in a chelating manner via the N bases to the alkaline-earth ions.

[a] W. Huadsai, Dr. L. Vendier, Dr. S. Bontemps
CNRS, Laboratoire de Chimie de Coordination (LCC)
Université de Toulouse
205 Route de Narbonne, BP 44099, F-31077 Toulouse Cedex 4, France
E-mail: sebastien.bontemps@lcc-toulouse.fr

[b] W. Huadsai, Dr. H. Görls, Prof. M. Westerhausen
Institute of Inorganic and Analytical Chemistry
Friedrich Schiller University Jena (FSU)
Humboldtstraße 8, D-07743 Jena, Germany
E-mail: m.we@uni-jena.de

[c] Dr. L. Magna
IFP Energies nouvelles (IFPEN)
Rond-Point de l'Échangeur de Solaize, 69360 Solaize, France

Supporting information for this article is available on the WWW under <https://doi.org/10.1002/ejic.202400128>

© 2024 The Authors. European Journal of Inorganic Chemistry published by Wiley-VCH GmbH. This is an open access article under the terms of the Creative Commons Attribution Non-Commercial NoDerivs License, which permits use and distribution in any medium, provided the original work is properly cited, the use is non-commercial and no modifications or adaptations are made.

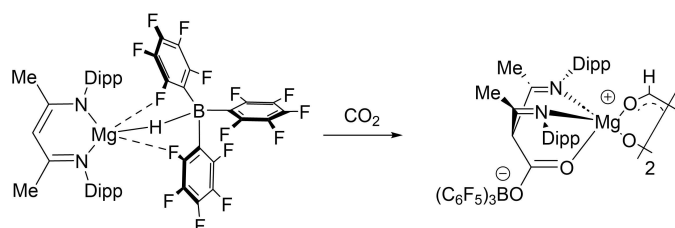
However, the binding of very bulky amidinato ions toward the softer calcium ion can vary significantly. For softer metal ions the aryl π -systems become suitable Lewis bases and hence are competitive with the rather hard N bases of the amidinato ion. Thus, the *anti*-conformation of the amidinato ligand releases steric strain within the amidinato ligand and is additionally stabilized by side-on coordination of an aryl substituent to the calcium ion.^[12,13] However, preparation of a stable amidinato calcium hydride requires a C-bound adamantyl group at the NCN-backbone.^[13] Amino groups at the carbon atom of the 1,3-diazaallyl anion (guanidates) are also suitable substituents for the synthesis of heteroleptic amidinato calcium complexes.^[14]

Enhancement of steric hindrance by larger diphenylmethyl substituents in *ortho* positions of the N-bound aryl groups finally ensures a low aggregation degree of hydrido magnesium species.^[15] Here, we study the reactivity of a bulky amidinato magnesium hydride with a C-bound adamantyl group at the backbone of the amidinato ion as stoichiometric and catalytic reductant toward carbon dioxide. Contrary to dinuclear β -diketiminato alkaline-earth metal hydrides of magnesium (I–Mg) and calcium (II–Ca) that have been studied earlier,^[14] the addition of CO₂ onto the backbone of the amidinato ligand can be excluded (see Scheme 1).^[16]

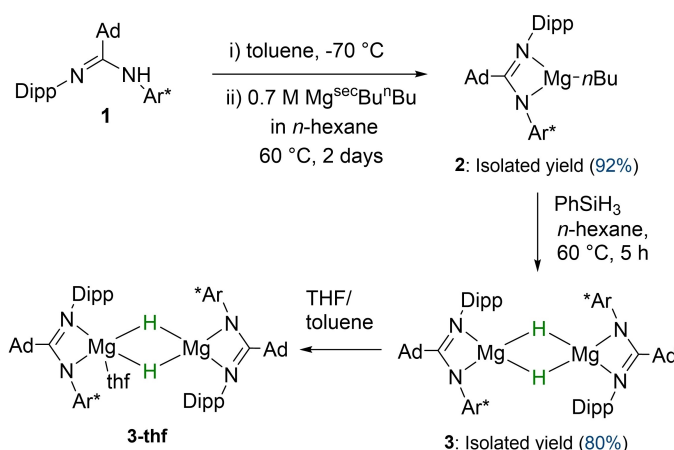
Results and Discussion

Synthesis and Reactivity of the Sterically Shielded Amidinato Magnesium Hydride

Following a previously reported procedure^[17] we prepared bulky amidine **1**, and subsequent metalation with dibutylmagnesium in hydrocarbons at 60 °C yielded the heteroleptic butylmagnesium amidinate **2** with a yield of 92%. The conversion of this compound with phenylsilane to the amidinato magnesium hydride **3** was performed in *n*-hexane at 60 °C within five hours with an isolated yield of 80% as depicted in Scheme 2. The dinuclear structure was maintained in toluene as had been shown by NMR experiments at different temperatures (Figure S13). The signal of the hydrido ligands remained unchanged whereas the signals of the *ortho*-diphenylmethyl substituents of the bulky aryl groups broadened at 233 K due to hindered rotation. The chemical shift of 3.85 ppm for the bridging hydrido ligands of **3** compare well with those of



Scheme 1. Stoichiometric reaction of I–Mg–B(C₆F₅)₃ with carbon dioxide via addition at the backbone of the nacnac ligand (carboxylate formation) and via formation of bridging formate ions (Dipp = C₆H₃-2,6-*i*Pr₂).



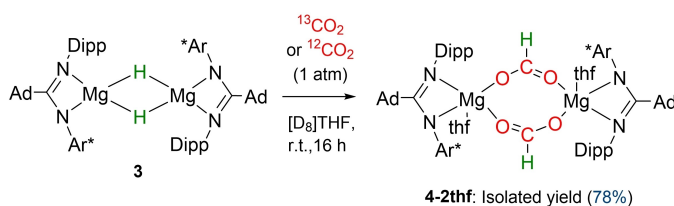
Scheme 2. Synthesis of the sterically encumbered amidinato magnesium hydride **3** via metalation of the corresponding amidine **1**, yielding butylmagnesium amidinate **2**, and subsequent conversion with phenylsilane to the hydrido complex **3**. Recrystallization from THF/toluene leads to formation of the thf adduct **3-thf**. (Ad = adamantyl, Dipp = C₆H₃-2,6-*i*Pr₂, Ar* = C₆H₃-2,6-(CHPh₂)₂).

dinuclear β -diketiminato magnesium hydrides with bridging hydrido ligands (3.8–3.9 ppm)^[6,17] whereas terminal Mg–H units show chemical shifts above 4 ppm.^[4,5]

Recrystallization from a mixture of THF and toluene gave single crystals of **3-thf**. Only one magnesium atom carried a thf ligand whereas the other one remained tetra-coordinated by the bidentate amidinato ligand and two hydrido bridges leading to different coordination numbers of the magnesium atoms.

The thf-free compound **3** reacted cleanly with 1 atm of CO₂ at room temperature in [D₈]THF yielding a single new species **4-2thf** within 16 hours as depicted in Scheme 3. In the ¹H NMR spectra, a singlet at $\delta(^1\text{H})=8.15$ ppm was detected for the formate residue when using ¹²CO₂ and a doublet resonance with ¹J_{CH}=206.9 Hz when employing ¹³C-enriched CO₂. The chemical ¹³C NMR shift was also in agreement with earlier reported values of Mg-bound formate analogues.^[18,19] The dinuclear structure of **4-2thf** was maintained in solution as verified by DOSY experiments. In the solid-state IR spectrum, a band at 1645 cm⁻¹ was observed for the C–O stretching vibration which shifted 50 cm⁻¹ to lower wave numbers for the ¹³C-labeled derivative [¹³C]**4-2thf**.

Removal of ligated thf ligands from **4-2thf** in vacuo destabilized this compound significantly and free amidine was



Scheme 3. Reaction of **3** with 1 atm of carbon dioxide at room temperature in THF yielding the dinuclear amidinato magnesium formate **4-2thf**.

liberated. Limited stability of such compounds had been observed earlier for the reduction of diisopropylcarbodiimide with a bulky amidinato magnesium hydride complex leading to the formation of the *N,N'*-diisopropylamidinato ligand, but this heteroleptic bis(amidinato) magnesium congener showed a very poor solution stability and degraded under formation of free amidine, too.^[6] In contrast, compound **4-2thf** was stable upon heating at 60 °C in [D₈]THF solution for more than 16 hours.

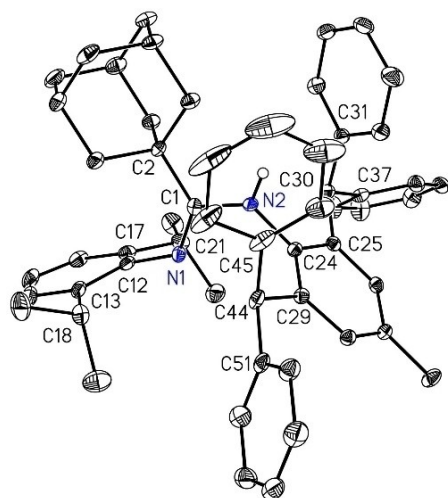


Figure 1. Molecular structure and atom labelling scheme of amidine **1**. The ellipsoids of the non-hydrogen atoms represent a probability of 30%, C-bound H atoms are neglected for the sake of clarity. Selected bond lengths (pm): N1-C1 129.1(4), N1-C12 141.0(4), N2-C1 136.4(4), N2-C24 143.5(4), N2-H1 84(3), C1-C2 155.1(4); bond angles (deg.): C1-N1-C12 126.4(3), C1-N2-C24 126.0(3), C1-N2-H1 120(2), C24-N2-H1 114(2), N1-C1-N2 117.4(3), N1-C1-C2 128.7(3), N2-C1-C2 113.8(3).

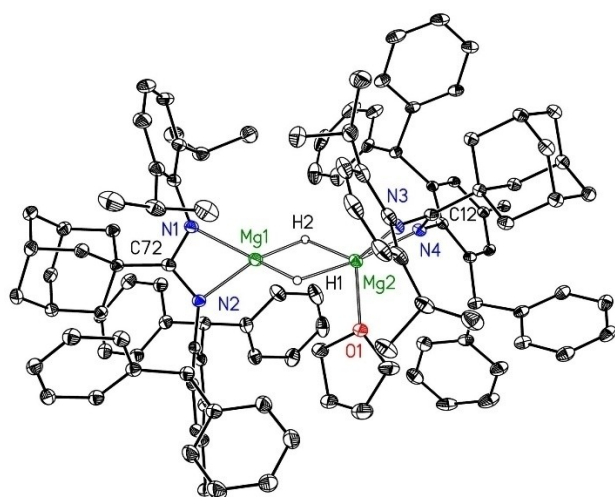


Figure 2. Molecular structure and atom labelling scheme of the amidinato magnesium hydride **3-thf**. The ellipsoids of the non-hydrogen atoms represent a probability of 30%, C-bound hydrogen atoms are omitted for clarity reasons.

Molecular Structures

To estimate the influence of steric hindrance on the molecules, we determined the crystal structures of the amidine **1** and the amidinato magnesium complexes **3-thf** and **4-2thf**.

Molecular structure and atom labelling scheme of the bulky amidine **1** are depicted in Figure 1 and Figure S21. The C1 and N2 atoms are in distorted trigonal planar environments with an *E*-configuration at the N1-C1 imine functionality due to steric reasons and hence, the *anti*-conformation is realized in the crystalline state. Distortions arise from the enormous steric hindrance between the bulky aryl and adamantyl substituents, leading to widened C–N–C bond angles. The vicinal hindrance between the adamantyl and Dipp groups significantly enhances the N1-C1-C2 and C1-N1-C12 bond angles. The adamantyl and C₆H₃-2,6-(CHPh₂)₂ substituents are *trans*-oriented to reduce steric hindrance, nevertheless, the C1-N2-C24 bond angle is enhanced, too.

The molecular structure and atom labelling scheme of the amidinato magnesium hydride **3-thf** are depicted in Figure 2 and Figure S22. Despite the large steric pressure, a *syn*-conformation of the N-bound bulky aryl groups is realized and the amidinato ligand acts as a bidentate chelating Lewis base. The magnesium atoms are in different coordination spheres: tetra-coordinate Mg1 adopts a distorted tetrahedral environment, whereas for the penta-coordinate Mg2 atom a τ -value of 0.47 is indicative for an intermediate coordination polyhedron between a distorted square pyramid and a trigonal bipyramid with N4 and H1 in axial positions ($\tau = (\alpha - \beta)/60^\circ$ with α as largest X-Mg2-Y and β as second largest X-Mg2-Y bond angles; $\tau = 1$ is indicative for a trigonal bipyramid and $\tau = 0$ for a square pyramid).^[20] The larger coordination number of Mg2 leads to longer Mg2-H1/2 bonds with the axial Mg2-H1 distance of 218 pm being larger than the equatorial Mg2-H2 value of 191 pm whereas tetra-coordinate Mg1 has bond lengths of 185 and 188 pm to H1 and H2, respectively. As expected, the amidinato ions have two very similar C–N bond lengths indicative of an ideal charge delocalization within the 1,3-diazaallylic moieties. Again, the axial Mg2-N4 bond length of 214.2(2) pm is significantly enhanced compared to the equatorial Mg2-N3 distance of 204.9(2) pm. For tetra-coordinate Mg1 rather similar Mg1-N1 and Mg1-N2 distances of 204.6(2) and 208.7(2) pm, respectively, are observed.

The molecular structure and atom labelling scheme of the centrosymmetric dinuclear amidinato magnesium formate **4-2thf** are depicted in Figure 3 and Figure S23. The Mg1 center carries an additional thf ligand and is penta-coordinate with a τ -value of 0.38 with the largest N2-Mg1-O3 bond angle of 156.77(8)°. Therefore, the axial Mg1-N2 bond length of 216.2(2) pm is larger than the Mg1-N1 distance of 209.6(2) pm. The *syn*-conformation of the amidinato ligand is maintained during formation of the bridging formate ion with equal C16-N1/2 bond lengths of 133.4(3) and 133.9(3) pm, respectively.

Selected bond lengths are summarized in Table 1. In the 1,3-diazaallylic system of amidine **1**, the C–N bond lengths differ by approx. 7 pm. In the deprotonated amidinate ions the C–N distances have very similar values indicative of an ideal

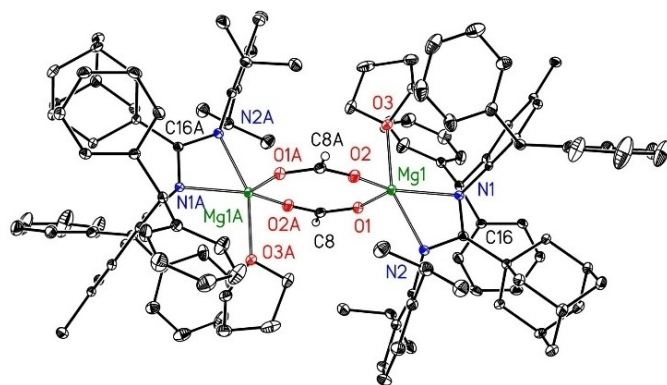


Figure 3. Molecular structure and atom labelling scheme of the amidinato magnesium formate **4-2thf**. Symmetry-related atoms are marked with the letter “A”. The ellipsoids of the non-hydrogen atoms represent a probability of 30%, the H atoms have been omitted for clarity reasons except those of the bridging formate ligands.

Table 1. Comparison of bond lengths (pm) of amidine **1** as well as the magnesium complexes **3-thf** and **4-2thf**.^[a]

	1	3-thf	3-thf	4-2thf
C.N.(Mg) ^[b]	–	4	5	5
Mg-N1 _{am}	–	204.6(2)	204.9(2)	209.6(2)
Mg-N2 _{am}	–	208.7(2)	214.2(2)	216.2(2)
Mg-H	–	186	205	–
Mg-O _{form}	–	–	–	195.1
Mg-O _{thf}	–	–	208.0(2)	213.5(2)
C _{am} -N1	129.1(4)	134.5(3)	134.5(3)	133.4(3)
C _{am} -N2	136.4(4)	135.2(3)	134.8(3)	133.9(3)
C _{am} -C _{Ad}	155.1(4)	154.7(4)	154.4(3)	155.0(3)
C _{Ad} -C _{am} -N1	128.7(3)	124.0(2)	127.1(2)	125.9(2)
C _{Ad} -C _{am} -N2	113.8(3)	125.9(2)	123.0(2)	124.1(2)
N1-C _{am} -N2	117.4(3)	109.9(2)	109.7(2)	110.0(2)

[a] Subscripts “Ad” (adamantyl), “am” (amidinate), “form” (formate), and “thf” (ligated tetrahydrofuran) denominate the position of the marked atom. [b] Coordination number of magnesium.

charge delocalization. The *anti*-conformation of amidine **1** allows significantly different C_{Ad}-C_{am}-N1/2 bond angles to release intramolecular steric strain. Deprotonation and coordination at magnesium ions stabilizes a *syn*-conformation with rather similar and widened C_{Ad}-C_{am}-N1/2 angles whereas a narrow N1-C_{am}-N2 bond angle is realized. Substitution of the very soft hydride bridge by rather hard formate ions enhances steric and electrostatic repulsion because the Mg-O_{form} values are smaller than the Mg-H bond lengths and in addition, the hydride ions are much more polarizable than oxygen bases. This repulsion leads to larger Mg-N distances to the amidinato chelate ligand and to larger Mg-O_{thf} distances.

Catalytic Reduction of Carbon Dioxide

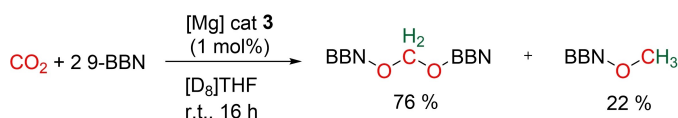
The dinuclear magnesium hydride **3** (1 mol-%, 0.013 mmol) was combined with 0.13 mmol of 9-BBN in 0.65 mL of [D₈]THF in an NMR tube and hexamethylbenzene was added as internal standard. Then the NMR tube was degassed and 1 atm of CO₂ was applied for three minutes at room temperature. The consumption of 9-BBN was monitored by ¹H and ¹³C{¹H} NMR spectroscopy. After 16 hours, 97% of 9-BBN was consumed yielding 76% of the bis(boryl)acetal (BBA) and 22% of the methoxyborane as depicted in Scheme 4.

The hydroboration of carbon dioxide with 9-BBN, using 1 mol-% of dinuclear *N,N'*-bis(diisopropylphenyl)-substituted β-diketiminato magnesium hydride under similar reaction conditions gave similar product ratios of BBA and methoxyborane but proceeded within 7 h 25 min.^[21] The decelerated hydroboration using catalytic amounts of amidinato magnesium hydride **3** was caused by the enhanced shielding of the hydrido ions by the bulkier N-bound aryl groups.

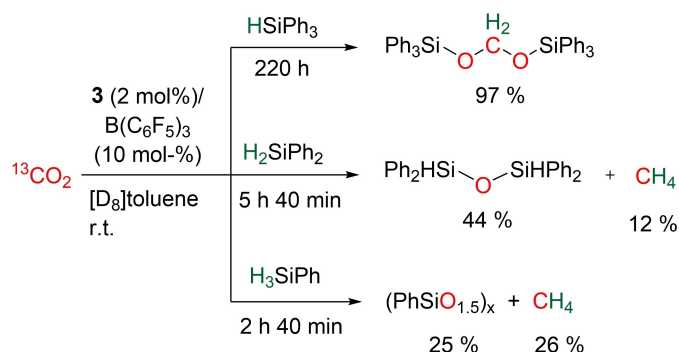
In a rather similar procedure, phenylsilanes H_{4-n}SiPh_n (n = 1, 2, and 3) and the standard mesitylene were added to a mixture of 2 mol-% of **3** and 10 mol-% of B(C₆F₅)₃ in [D₈]toluene in an NMR tube. The addition of B(C₆F₅)₃ was mandatory because neither the hydrido magnesium species nor B(C₆F₅)₃ alone catalyzed the hydrosilylation reaction. An excess of the highly Lewis-acidic perfluorinated triphenylborane was applied to allow activation of the magnesium hydride and of the silane. The atmosphere was exchanged by 1 atm of ¹³C-labeled carbon dioxide. The conversion was monitored by ¹H and ¹³C NMR spectroscopy at different time intervals. The products were identified by comparison of their chemical shifts with literature values.

Under these reaction conditions, triphenylsilane (n = 3) reacted within 220 hours at room temperature quantitatively to the bis(triphenylsilyl)acetal (Ph₃SiO)₂CH₂ as depicted in Scheme 5. Application of less shielded diphenylsilane (n = 2) enhanced the reactivity and already after 5 h 40 min significant amounts of [¹³C]methane (12%) evolved whereas 44% of 1,1,3,3-tetraphenyldisiloxane (HPh₂Si)₂O were present in the reaction mixture. The distinct signals of ¹³CH₄ were monitored at δ(¹H) = 0.21 as a doublet (J_{CH} = 125.6 Hz) and at δ(¹³C) = –4.4 as a quintet with the same coupling constant. The use of phenylsilane (n = 1) enhanced the rate of conversion again and already after 2 h 40 min 26% of [¹³C]methane was detected. In addition, the formation of 25% of the silsesquioxane (PhSiO_{1.5})_x showed that all Si-bound hydrogen atoms reacted.

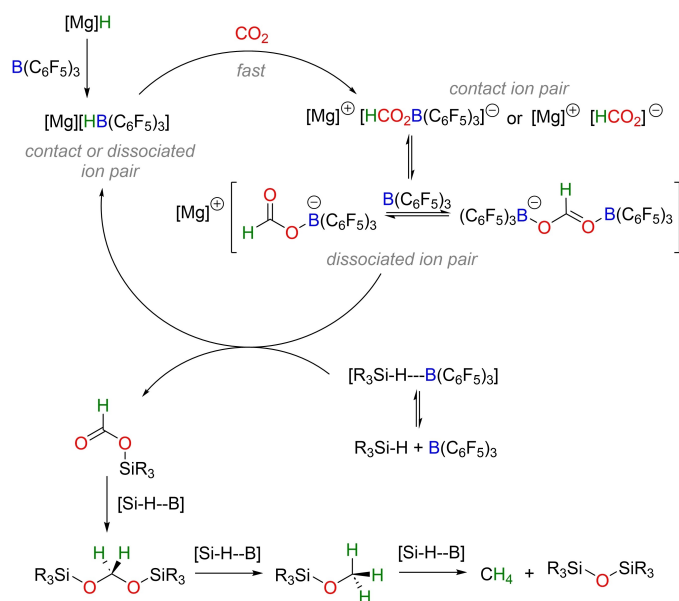
The proposed mechanism is depicted in Scheme 6. As shown earlier for a bulky β-diketiminato magnesium hydride,



Scheme 4. Catalytic reduction of carbon dioxide with 9-BBN, using 1 mol-% of catalyst **3**, yielding 76% of bis(boryl)acetal and 22% of methoxyborane after 16 hours at room temperature.



Scheme 5. Catalytic reduction of carbon dioxide with phenylsilanes $H_{4-n}SiPh_n$ ($n = 1, 2,$ and 3), using 2 mol-% of catalyst **3** together with 10 mol-% of $B(C_6F_5)_3$ in $[D_8]$ toluene at room temperature.



Scheme 6. Proposed mechanism of hydrosilylation of carbon dioxide catalyzed by amidinato magnesium hydride $[Mg]H$ (**3**) in the presence of excess $B(C_6F_5)_3$ which activates both $[Mg]H$ and silane.

strong Lewis bases can deaggregate dinuclear complexes.^[5] Therefore, 1H DOSY NMR experiments were performed in toluene and in THF. In toluene, a hydrodynamic radius of 970 pm was determined whereas in THF a smaller value of 750 pm was hinting toward a fast monomer-dimer equilibrium.

Based on our blank experiments that neither the hydrido magnesium complex nor $B(C_6F_5)_3$ alone could catalyze hydrosilylation reactions we exclude the direct insertion of CO_2 into the $Mg-H$ bond of catalyst **3** but formation of intermediate amidinato magnesium borate $[Mg][HB(C_6F_5)_3]$ is assumed. This observation agrees well with earlier findings of Rauch and Parkin.^[16b] The addition of carbon dioxide immediately yields the formatoborate species either as contact ion pair or as dissociated ions. In a subsequent step, silyl formate is released via the nucleophilic attack of the formate oxygen atom at the silicon of the activated silane $R_3Si-H \cdots B(C_6F_5)_3$ leading to the regeneration of the magnesium hydride catalyst.

After formation of the initial silyl formate rapid hydrosilylation finally yields siloxanes and methane via intermediate bis(silyl)acetal and methoxysilane. The bis(silyl)acetal has only been isolated if rather bulky triphenylsilane has been applied leading to rather slow conversion kinetics. The methoxysilane intermediate has not been found in this study but methoxyborane has been observed during hydroboration of CO_2 as discussed above (see also Scheme 4). Hydrosilylation with less shielded silanes yields siloxanes and methane within a few hours at ambient temperature.

Conclusions

The sterically encumbered amidinato magnesium hydride **3** is accessible by a straightforward procedure with a good yield via metalation of the amidine **1** with dibutylmagnesium; isolation of the intermediately formed butylmagnesium amidinate **2** is unnecessary. The hydride ions in **3** occupy bridging positions between two magnesium centers. The constriction induced by the extremely bulky N-bound aryl groups allows only the coordination of one thf co-ligand at the dinuclear complex, leading to **3-thf** with one tetra- and another penta-coordinate Mg center. In THF solution, carbon dioxide readily inserts into the $Mg-H$ bonds yielding dinuclear amidinato magnesium formate **4-2 thf**.

Hydride **3** can act as an efficient hydroboration catalyst in the addition reaction of 9-BBN onto carbon dioxide yielding bis(boryl)acetal and methoxyborane. In a similarly performed catalytic hydrosilylation reaction of CO_2 this amidinato magnesium hydride **3** is inactive. Addition of excess of perfluorinated triphenylborane activates the hydrido magnesium complex **3** as well as the silane. Depending on the substitution degree of phenylsilane $H_{4-n}SiPh_n$ ($n = 1, 2,$ and 3), bis(silyl)acetals ($n = 3$) or siloxanes ($n = 1$ and 2) and methane have been observed. A decreasing number of phenyl groups strongly accelerates the catalytic hydrosilylation reaction.

Experimental

General: All reactions involving air- and moisture-sensitive compounds were carried out using standard Schlenk line and glovebox techniques in an atmosphere of either anhydrous nitrogen or argon. Solvents were either dried over KOH and then distilled over sodium/benzophenone under nitrogen atmosphere or employed on an MBraun SPS column prior to use. Deuterated solvents were either dried over sodium, degassed, and distilled under a nitrogen atmosphere and stored under nitrogen with sodium or freeze-pump-thaw, degassed and stored under argon over 4 Å molecular sieves. All substrates were purchased from Alfa Aesar, abcr, SigmaAldrich, or TCI and used without further purification. The substrate for the synthesis of amidine **1**, $O=C(Ad)-NH-C_6H_2-4-Me-2,6-(CHPh)_2$, was prepared according to a literature protocol.^[22] The purity of the compounds was controlled by NMR spectroscopy. Quick Pressure Valve NMR tubes were used for the reactions with CO_2 . NMR experiments were conducted in pressurizable NMR tubes. 1H and $^{13}C\{^1H\}$ NMR spectra were recorded on Bruker Avance III 400 (BBO, BBFO probes), Avance II HD 500 (BBO Prodigy probe), and Avance neo 500 (BBFO Prodigy probe) spectrometers. Chemical

shifts are reported in parts per million and coupling constants in Hz, relative to SiMe₄ for ¹H and ¹³C analyses as external standard.

Synthesis of amidinato magnesium hydride 3: In a 150 ml Schlenk flask, a 0.7 M solution of ⁿBu^sBuMg in *n*-hexane (5 ml, 3.30 mmol) was added dropwise to a toluene solution (60 ml) containing compound 1 (2.50 g, 3.30 mmol). The reaction was heated to 70 °C for 2 days. Thereafter, the reaction mixture was cooled to ambient temperature, and the solvent was removed *in vacuo*, resulting in sticky yellowish residues. The residues were washed twice with *n*-hexane (20 ml), resulting in a white precipitate, which was filtered and dried in high vacuum and yielding compound 2 (yield: 2.54 g, 92%).

Then, product 2 was re-dissolved in toluene (20 ml), and PhSiH₃ (1 ml, 7.26 mmol) was added dropwise at 273 K. The reaction was maintained at room temperature for 20 min prior to heating to 65 °C for 5 h. Then the reaction was cooled and filtered. All volatiles were removed *in vacuo*, and 40 ml of *n*-hexane was added under vigorous stirring for 2 h, resulting in a white precipitate. The suspension was filtered yielding a white solid, which was washed with cold *n*-hexane (60 ml) to remove unreacted PhSiH₃ and by-products (PhSiH₂*n*Bu) giving compound 3 (yield: 2.0 g, 80%). Colorless crystals of 3-thf suitable for X-ray diffraction experiments were grown after cooling of a saturated mixture of toluene/THF at -40 °C overnight (yield: 28 mg, 64%).

Physical data of 2: ¹H NMR (400 MHz, 298 K, C₆D₆): δ = -1.09 (t, ³J_{HH} = 6 Hz, 2H, Mg-CH₂), 0.92 (m, 3H, Mg-CH₃), 1.16 (d, ³J_{HH} = 6 Hz, 6H, Dip-CH(CH₃)₂), 1.15 (overlap with Dipp-CH₃, m, 4H, Mg-CH₂), 1.34 (d, ³J_{HH} = 6 Hz, 6H, Dip-CH₃), 1.45 (m, 6H, Ad-H), 1.78 (s, 3H, Ad-H), 1.93 (d, ³J_{HH} = 6 Hz, 3H, Ar*-CH₃), 2.32 (s, 6H, Ad-H), 3.55 (sept, ³J_{HH} = 6 Hz, 2H, Dip-CH), 6.18 (s, 2H, CH-Ph₂), 6.87 (s, 2H, Ar* m-Ar-H), 7.00–7.33 (m, 23H, Ar-H). ¹³C{¹H} NMR (100 MHz, 298 K, C₆D₆): δ = 6.2 (Mg-CH₂), 14.2 (Mg-CH₃), 21.3, 21.5, 22.0, (CH₃), 26.1, 28.9 (CH), 29.2 (Ad-C), 31.5 (ⁿBu-CH₂), 31.7 (ⁿBu-CH₂), 36.7, 40.4, 47.1 (Ad-C), 53.9 (CH-Ph₂), 123.0, 124.1, 126.1, 126.9, 128.5, 130.0, 130.3, 131.7, 138.7, 142.2, 143.5, 144.4 (Ar-C), 175.6 (NCN). **M.p.** 240.2–242.1 °C; **Anal. calc.** for C₆₀H₈₈MgN₂: C 85.64, H 8.15, N 3.33; **found:** C 85.24, H 8.12, N 3.32. **MS/ESI m/z:** 760.48 (1 + H⁺). **IR (solid, ν/cm⁻¹):** 1600 (m), 1480 (m), 1437 (s), 1368 (vs), 1344 (s), 1264 (w), 1112 (w), 1077 (w), 1032 (w), 830 (w), 804 (m), 760 (s), 699 (vs), 604 (m), 554 (m), 541 (m).

Physical data of 3-thf: ¹H NMR (400 MHz, 298 K, C₆D₆): δ 0.97 (m, 6H, Ad-H), 1.06 (d, ³J_{HH} = 6.7 Hz, 12H, Dip-CH₃), 1.18 (m, 9H, Ad-H), 1.32 (d, ³J_{HH} = 6.8 Hz, 12H, Dip-CH₃), 1.47 (m, 9H, Ad-H), 1.73 (m, 6H, Ad-H), 2.07 (s, 6H, CH₃), 3.60 (sept, ³J_{HH} = 7.0 Hz, 4H, Dip-CH), 3.85 (s, 2H, Mg-H), 6.32 (s, 4H, CH^d-Ph₂), 6.94 (m, 10H, Ar-H), 7.03–7.09 (m, 15H, Ar-H), 7.21 (m, 10H, Ar-H), 7.48 (m, 15H, Ar-H). ¹³C{¹H} NMR (101 MHz, 298 K, C₆D₆): δ 21.3 (CH₃), 21.9, 25.7 (CH₃), 28.4 (Ad-C), 28.8 (CH^d), 36.1, 36.2, 38.7 (Ad-C), 46.0 (Ad-C^{IV-9}), 53.2 (CH^d-Ph₂), 123.1, 124.1, 126.8, 128.8, 128.9, 129.6, 130.0, 130.4 (Ar-C), 135.6 (Ar-C^{IV}), 136.9 (Ar-C), 139.4 (Ar-C^{IV}), 141.6 (Ar-C^{IV-m}), 142.7 (Ar-C^{IV-p}), 143.8 (Ar-C^{IV}), 145.8 (Ar-C^{IV}), 177.6 (NCN). **¹H DOSY** (600 MHz, 298 K, toluene-*d*₈): D = 3.76 × 10⁻¹⁰ m² s⁻¹; R_H = 9.67 Å. **M.p.** > 260 °C; **Anal. calc.** for C₁₁₂H₁₂₀Mg₂N₄: C 85.64, H 7.70, N 3.09; **found:** C 83.88, H 7.70, N 3.21. **MS/ESI m/z:** 761.4858 (1 + H⁺). **IR ν/cm⁻¹ (ATR):** 3084 (w), 3061 (w), 3026 (w), 2961 (w), 2906 (w), 2850 (w), 1599 (w), 1494 (w), 1436 (m), 1388 (s), 1368 (m), 1314 (w), 1264 (w), 1237 (vw), 1191 (vw), 1144 (vw), 1112 (w), 1077 (w), 1061 (w), 1032 (w), 981 (vw), 956 (vw), 933 (vw), 916 (vw), 883 (vw), 861 (w), 829 (vw), 799 (w), 759 (m), 724 (w), 700 (s), 651 (w).

Synthesis of amidinato magnesium formate 4-2thf: In a pressurized NMR tube, a solution of compound 3 (15 mg, 0.025 mmol) in [D₈]THF (0.5 ml) was degassed and exposed to 1 atm of dynamic CO₂ for 3 min. The sample was sealed and maintained at ambient

temperature for 16 h before the NMR spectra were recorded. The full conversion of 3 to 4-2thf was monitored by ¹H NMR spectroscopy. ¹H DOSY and 2D NMR experiments were recorded after 48 h of the reaction time. Under a CO₂ atmosphere, colorless crystals of 4-2thf precipitated at 25 °C in a sealed NMR tube. The crystals were collected by filtration in a glovebox and washed twice with cold [D₈]THF (Yield: 15.5 mg, 78%).

Physical data of 4-2thf: ¹H NMR (400 MHz, 298 K, [D₈]THF): δ 0.94 (m, 6H, Ad-H), 1.11 (m, 6H, Ad-H), 1.17 (d, ³J_{HH} = 6.7 Hz, 12H, Dip-CH₃), 1.27 (d, ³J_{HH} = 6.6 Hz, 12H, Dip-CH₃), 1.33 (m, 18H, Ad-H), 2.21 (s, 6H, CH₃), 3.65 (sept, ³J_{HH} = 7.0 Hz, 4H, Dip-CH), 6.24 (s, 4H, CH^d-Ph₂), 6.85 (m, 2H, Dip-Ar-H), 6.94 (m, 4H, Ar-H), 7.03–7.07 (m, 8H, Ar-H), 7.13 (t, ³J_{HH} = 7.3 Hz, 12H, Ar-H), 7.23–7.28 (m, 16H, Ar-H), 7.33–7.35 (m, 8H, Ar-H), 8.15 (s, 2H, Mg-CHO). ¹³C{¹H} NMR (101 MHz, 298 K, [D₈]THF): δ 21.4 (CH₃), 23.4, 27.9 (Dip-CH₃), 28.9 (Ad-C), 29.4 (Dip-CH), 36.3, 39.5 (Ad-C), 46.6 (Ad-C^{IV-9}), 52.5 (CH^d-Ph₂), 123.6, 123.8, 126.5, 126.7, 128.8, 129.0, 129.3, 130.0, 130.7, 130.9 (Ar-C), 136.9 (Ar-C^{IV}), 143.7 (Ar-C^{IV-m}), 144.8 (Ar-C^{IV}), 146.2 (Ar-C^{IV-p}), 147.6 (Ar-C^{IV}), 148.5 (Ar-C^{IV}), 169.8 (Mg-C), 177.1 (NCN). **¹H DOSY** (600 MHz, 298 K, THF-*d*₈): D = 4.42 × 10⁻¹⁰ m² s⁻¹; R_H = 9.87 Å. **M.p.** 235–237 °C; **Anal. calc.** for C₁₂₂H₁₃₆Mg₂N₄O₆: C 81.27, H 7.60, N 3.11; **found:** C 80.25, H 7.59, N 2.96. The elemental C and N data were found to be inaccurate despite multiple attempts. A more accurate agreement was achieved by including additional 1.5 to 2 molecules of THF in the calculated chemical formula of 4-2thf. It is noteworthy mentioning that compound 4-2thf underwent decomposition under vacuum and attempts to thoroughly dry the crystals to obtain more precise CHN values were unsuccessful. **HRMS (ESI⁺) m/z: calc** 761.4867 (1 + H⁺), **found** 761.4858 (1 + H⁺). **IR (ATR, ν/cm⁻¹) of [¹³C]4-2thf:** 3059 (vw), 2984 (vw), 2957 (w), 2900 (w), 2871 (w), 2848 (w), 2236 (w), 2081 (w), 1595 (s, νO₂C), 1492 (m), 1463 (w), 1433 (s), 1397 (vs), 1375 (s), 1343 (w), 1311 (w), 1265 (w), 1250 (w), 1229 (w), 1206 (w), 1191 (w), 1177 (w), 1154 (w), 1129 (vw), 1096 (m), 1077 (w), 1044 (s), 1003 (m), 949 (w), 885 (vw), 862 (w), 841 (w), 827 (w), 808 (w), 795 (vw), 758 (s), 741 (s), 698 (vs). **IR (ATR, ν/cm⁻¹) of [¹²C]4-2thf:** 3058 (vw), 3024 (vw), 3009 (vw), 2957 (w), 2904 (w), 2876 (w), 1645 (s, νO₂C), 1597 (w), 1493 (m), 1462 (w), 1434 (m), 1400 (vs), 1392 (vs), 1369 (m), 1343 (w), 1324 (vw), 1311 (w), 1293 (vw), 1281 (vw), 1266 (w), 1249 (vw), 1230 (w), 1212 (vw), 1192 (w), 1179 (w), 1154 (w), 1132 (vw), 1110 (w), 1103 (w), 1078 (w), 1064 (vw), 1054 (vw), 1040 (vw), 1032 (w), 1001 (m), 964 (vw), 951 (w), 933 (vw), 923 (vw), 915 (w), 882 (vw), 861 (w), 829 (w), 759 (m), 746 (m), 715 (m), 698 (vs), 681 (m).

Crystal structure determinations.^[23] The intensity data for the compounds 1 and 4-2thf were collected on a Nonius KappaCCD diffractometer using a Mo-Kα μs microfocus source and an Apex2 CCD detector. Data were corrected for Lorentz and polarization effects; absorption was taken into account on a semi-empirical basis using multiple-scans.^[24–27] The single crystal X-ray diffraction data of 3-thf were recorded on a XtaLAB Synergy, Dualflex, HyPix diffractometer with Hybrid Pixel Array detector from Rigaku Oxford Diffraction applying a mirror monochromatic Cu Kα radiation (λ = 1.54184 Å). Analytical absorption corrections were applied to the data.^[28] The structures were solved by intrinsic methods (SHELXT^[29]) and refined by full-matrix least squares techniques against F_o² (SHELXL-2018^[30]). The hydrogen atoms bonded to the amine group of N2 of 1 and both hydride atoms H1 and H2 of compound 3-thf were located by difference Fourier synthesis and refined isotropically. All other hydrogen atoms were included at calculated positions with fixed thermal parameters. The crystal of 4-2thf contains large voids, filled with disordered solvent molecules. The size of the voids is 1315 Å³/unit cell. Their contribution to the structure factors was secured by back-Fourier transformation using the SQUEEZE routine of the program PLATON^[31] resulting in 339 electrons/unit cell. All non-hydrogen atoms were refined

anisotropically.^[30] Crystallographic data as well as structure solution and refinement details are summarized in Table S1. XP was used for structure representations.^[32]

Supporting Information

Experimental details of the synthesis of amidine **1**, NMR and IR spectra of all new compounds, crystallographic and refinement data, kinetic studies on catalytic hydroboration and hydrosilylation of CO₂. The CIF files of the X-ray structure determinations have been deposited at CCDC.^[23]

Acknowledgements

This research has received funding from the European Union's Horizon 2020 research and innovation programme under the Marie Skłodowska-Curie grant agreement No. 860322. We acknowledge the valuable support of the NMR service platforms at LCC Toulouse, France, and of the Faculty of Chemistry and Earth Sciences of the FSU Jena, Germany. Open Access funding enabled and organized by Projekt DEAL.

Conflict of Interests

The authors declare no conflict of interest.

Data Availability Statement

The data that support the findings of this study are available in the supplementary material of this article.

Keywords: amidinato magnesium complexes · CO₂ activation · hydrido magnesium complexes · hydroboration · hydrosilylation

- [1] a) L. J. Murphy, K. N. Robertson, R. A. Kemp, H. M. Tuononen, J. A. Clyburne, *Chem. Commun.* **2015**, 51, 3942–3956; b) A. Paparo, J. Okuda, *Coord. Chem. Rev.* **2017**, 334, 136–149.
- [2] a) S. Bontemps, *Coord. Chem. Rev.* **2016**, 308, 117–130; b) K. A. Grice, *Coord. Chem. Rev.* **2017**, 336, 78–95; c) N. A. Tappe, R. M. Reich, V. D'Elia, F. E. Kühn, *Dalton Trans.* **2018**, 47, 13281–13313; d) J. S. Jestilä, E. Uggerud, *Organometallics* **2021**, 40, 1735–1743.
- [3] a) S. Aldridge, A. J. Downs, *Chem. Rev.* **2001**, 101, 3305–3365; b) S. Harder, *Chem. Commun.* **2012**, 48, 11165–11177.
- [4] M. Arrowsmith, B. Maitland, G. Kociok-Köhn, A. Stasch, C. Jones, M. S. Hill, *Inorg. Chem.* **2014**, 53, 10543–10552.
- [5] S. J. Bonyhady, C. Jones, S. Nembenna, A. Stasch, A. J. Edwards, G. J. McIntyre, *Chem. Eur. J.* **2010**, 16, 938–955.
- [6] C. Bakewell, *Dalton Trans.* **2020**, 49, 11354–11360.
- [7] a) F. T. Edelmann, *Adv. Organomet. Chem.* **2008**, 57, 183–352; b) T. Chlupaty, A. Růžicka, *Coord. Chem. Rev.* **2016**, 314, 103–113.

- [8] P. C. Andrews, M. Brym, C. Jones, P. C. Junk, M. Kloth, *Inorg. Chim. Acta* **2006**, 359, 355–363.
- [9] J. A. R. Schmidt, J. Arnold, *J. Chem. Soc. Dalton Trans.* **2002**, 2890–2899.
- [10] a) R. T. Boéré, M. L. Cole, P. C. Junk, *New J. Chem.* **2005**, 29, 128–134; b) G. J. Moxey, F. Ortu, L. G. Sidley, H. N. Strandberg, A. J. Blake, W. Lewis, D. L. Kays, *Dalton Trans.* **2014**, 43, 4838–4846; c) C. Loh, S. Seupel, H. Görls, S. Kriek, M. Westerhausen, *Eur. J. Inorg. Chem.* **2014**, 1312–1321; d) I. V. Basalov, O. S. Yurova, A. V. Cherkasov, G. K. Fukin, A. A. Trifonov, *Inorg. Chem.* **2016**, 55, 1236–1244.
- [11] N. Nimitsiriwat, V. C. Gibson, E. L. Marshall, P. Takolpuckdee, A. K. Tomov, A. J. P. White, D. J. Williams, M. R. J. Elsegood, S. H. Dale, *Inorg. Chem.* **2007**, 46, 9988–9997.
- [12] a) A. Causero, H. Elsen, G. Ballmann, A. Escalona, S. Harder, *Chem. Commun.* **2017**, 53, 10386–10389; b) A. Causero, H. Elsen, J. Pahl, S. Harder, *Angew. Chem. Int. Ed.* **2017**, 56, 6906–6910; c) S. Brand, A. Causero, H. Elsen, J. Pahl, J. Langer, S. Harder, *Eur. J. Inorg. Chem.* **2020**, 1728–1735.
- [13] A. Causero, G. Ballmann, J. Pahl, H. Zijlstra, C. Färber, S. Harder, *Organometallics* **2016**, 35, 3350–3360.
- [14] C. Glock, C. Loh, H. Görls, S. Kriek, M. Westerhausen, *Eur. J. Inorg. Chem.* **2013**, 3261–3269.
- [15] W. Huadsai: Activation of Carbon Dioxide with Highly Lewis Acidic Compounds, *PhD thesis*, Friedrich Schiller University Jena (Germany), **2024**.
- [16] a) M. D. Anker, M. Arrowsmith, P. Bellham, M. S. Hill, G. Kociok-Köhn, D. J. Liptrot, M. F. Mahon, C. Weetham, *Chem. Sci.* **2014**, 5, 2826–2830; b) M. Rauch, G. Parkin, *J. Am. Chem. Soc.* **2017**, 139, 18162–18165.
- [17] C. N. de Bruin-Dickason, T. Sutcliffe, C. Alvarez Lamsfus, G. B. Deacon, L. Maron, C. Jones, *Chem. Commun.* **2018**, 54, 786–789.
- [18] M. D. Anker, M. Arrowsmith, P. Bellham, M. S. Hill, G. Kociok-Köhn, D. J. Liptrot, M. F. Mahon, C. Weetham, *Chem. Sci.* **2014**, 5, 2826–2830.
- [19] a) S. Schnitzler, T. P. Spaniol, L. Maron, J. Okuda, *Chem. Eur. J.* **2015**, 21, 11330–11334; b) S. Schnitzler, T. P. Spaniol, J. Okuda, *Inorg. Chem.* **2016**, 55, 12997–13006; c) L. E. Lemmerz, A. Wong, G. Ménard, T. P. Spaniol, J. Okuda, *Polyhedron* **2020**, 178, 114331.
- [20] A. W. Addison, T. N. Rao, J. Reedijk, J. Van Rijn, G. C. Verschoor, *J. Chem. Soc., Dalton Trans.* **1984**, 1349–1356.
- [21] W. Huadsai, M. Westerhausen, S. Bontemps, *Organometallics* **2023**, 42, 2921–2926.
- [22] B. Rezaei Kheirkhah, W. Huadsai, P. Liebing, S. Bontemps, M. Westerhausen, *Organometallics* **2023**, 42, 2304–2311.
- [23] Deposition numbers CCDC-2334211 (for **1**), 2334212 (for **3-thf**), and 2334213 (for **4-2thf**) contain the supplementary crystallographic data for this paper. These data are provided free of charge by the joint Cambridge Crystallographic Data Centre and Fachinformationszentrum Karlsruhe Access Structures service.
- [24] R. Hooft, *COLLECT, Data Collection Software*, Nonius B. V., Netherlands, **1998**.
- [25] Z. Otwinowski, W. Minor, in *Methods in Enzymology* (Eds. C. W. Carter, R. M. Sweet), vol. 276, part A, Academic Press, San Diego, USA, **1997**, pp. 307–326.
- [26] a) *SADABS 2.10*, Bruker-AXS Inc. **2002**, Madison, WI, USA; b) *SADABS 2016/2*: L. Krause, R. Herbst-Irmer, G. M. Sheldrick, D. Stalke, *J. Appl. Crystallogr.* **2015**, 48, 3–10.
- [27] Bruker APEX4 Bruker AXS LLC, Madison, WI, USA, **2021**.
- [28] *CrysAlis PRO 1.171.41.120a* (Rigaku Oxford Diffraction), **2021**.
- [29] G. M. Sheldrick, *Acta Crystallogr. Sect. A* **2015**, 71, 3–8.
- [30] G. M. Sheldrick, *Acta Crystallogr. Sect. C* **2015**, 71, 3–8.
- [31] A. L. Spek, *Acta Crystallogr. Sect. C* **2015**, 71, 9–18.
- [32] XP, Siemens Analytical X-ray Instruments Inc., Karlsruhe, Germany, **1990**; Madison, WI, USA, **1994**.

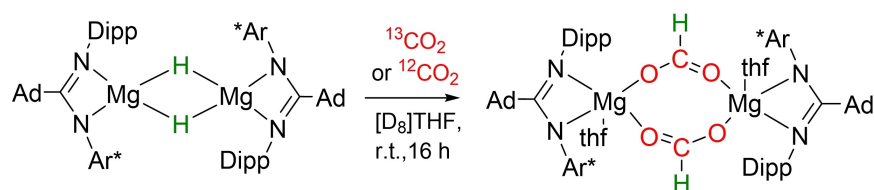
Manuscript received: March 6, 2024

Revised manuscript received: April 24, 2024

Accepted manuscript online: April 25, 2024

Version of record online: ■■, ■■

RESEARCH ARTICLE



Bulky amidinate ligands prevent Schlenk-type ligand scrambling in magnesium complexes allowing the synthesis of an amidinato magnesium hydride (Ad = adamantyl, Ar* = C₆H₂-4-Me-2,6-(CHPh₂)₂, Dipp = C₆H₃-2,6-

*i*Pr₂). Carbon dioxide can be inserted into the Mg–H bonds yielding formate derivatives. In addition, this hydrido magnesium species is a highly efficient hydroboration and hydrosilylation catalyst.

W. Huadsai, Dr. L. Vendier, Dr. H. Görls, Dr. L. Magna, Dr. S. Bontemps*, Prof. M. Westerhausen*

1 – 8

Stoichiometric and Catalytic Reduction of Carbon Dioxide by a Sterically Encumbered Amidinato Magnesium Hydride

